Journal of Physics and Its Applications

Journal homepage : https://ejournal2.undip.ac.id/index.php/jpa/index

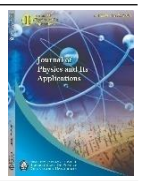

Analysis of Total Proton Therapy Dose Distribution with Pencil Beam Collimator Model and Varied Beam Directions in Craniopharyngioma Tumor using MCNP6 Software

Widia Hayati[1*], Utari[1], Fuad Anwar[1], Suharyana[1], Fajar Arianto[2], and Azizul Khakim[3]

[1]*Department of Physics, Faculty of Mathematics and Natural Science, Universitas Sebelas Maret, Surakarta, Indonesia*
[2]*Department of Physics, Faculty of Science and Mathematics, Universitas Diponegoro, Semarang, Indonesia*
[3]*Nuclear Energy Regulatory Agency, Jakarta, Indonesia*

**corresponding author: widianurh19@student.uns.ac.id*

ARTICLE INFO

Article history:
Received: 24 July 2024
Accepted: 6 November 2024
Available online: 30 November 2024

Keywords:
Proton Therapy
Craniopharyngioma
Pencil Beam
Beam Direction
MCNP6 Software

ABSTRACT

Proton therapy modeling for treating craniopharyngioma tumors was conducted using a pencil beam collimator, and variations in beam directions were performed using MCNP6 software. The simulation was carried out on a head and neck phantom with the tumor cells modeled within a cubic irradiation area geometry with a 1.2 cm side length, divided into 27 small cubic voxels with a small voxel side length of 0.4 cm. The radiation source from the irradiation area's right, left, and top directions, with a diameter of 0.4 cm, was directed at each cubic voxel. Variation in radiation source directions indicated that irradiation from the right direction of the irradiation area is the most recommended approach, with a dose uniformity level of 83.47%. Healthy organs surrounding the irradiation area received lower doses than those obtained by tumor cells, and the majority remained below the Organ At Risk (OAR) threshold. Healthy organs received the highest dose, particularly in the brain region, at a relative 0.46% compared to the total dose received by tumor cells.

1. Introduction

Craniopharyngioma is a rare tumor that grows in the brain with a low histological grade (WHO I). Craniopharyngioma is considered a benign tumor, but it is locally invasive, and both the disease and the treatments used to control it can carry long-term morbidity risks [1]. Craniopharyngioma accounts for 1.2 - 4.6% of all intracranial tumors and can occur at any age without gender differences [2]. Symptoms that may appear in patients with craniopharyngioma include a combination of endocrine, visual, cognitive, and symptoms due to increased intracranial pressure.

Proton therapy is an alternative radiation therapy with advantages, where the radiation emitted can be focused on the tumor cells while sparing the surrounding healthy cells [3]. Proton therapy has physical properties that allow for a rapid dose drop-off beyond the target depth, known as the Bragg peak [4]. Proton therapy delivery methods are generally divided into two categories: Passive Scattering Proton Therapy (PSPT) and Pencil Beam Scanning (PBS). PSPT spreads proton beams into uniform beams through single scattering for smaller field sizes and double scattering for larger field sizes. At the same time, PBS is performed by passing the proton beams through filters that control energy [5]. Following the tumor's shape, the distribution of PBS ensures that the radiation does not exceed the target volume boundaries, with the maximum dose being delivered only to the tumor [6].

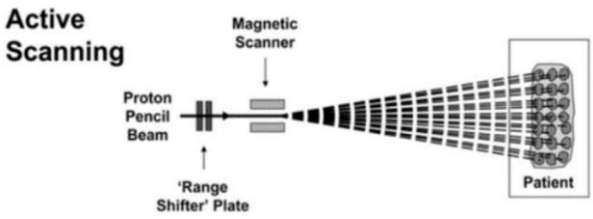

Fig. 1: Illustration of pencil beam (active) scanning on proton therapy.

Tumor treatment is carried out through a series of treatment planning systems (TPS) to ensure the precise delivery of radiation doses to kill cancer cells while reducing the dose that healthy surrounding cells can receive. Simulation using the Monte Carlo method is used to evaluate the quality of proton beams by calculating the dose profiles delivered by energetic protons. The Monte Carlo method can be simulated through the MCNP application, which provides results based on particle interactions in complex geometry structures and their constituent materials. Results obtained through this method are considered superior to the analytical algorithms commonly used to model dose distributions for treatment [7,8].

Cancer modeling with MCNP-based simulation has been done at the Physics Study Program, FMIPA UNS. Putri [9] demonstrated the proton therapy model in craniopharyngioma cancer with a PBS model using MCNP6 software. The energy used in the study was in the range of 108 - 115 MeV. The results showed an isodose rate of 86.35% with a dose

received by healthy cells of (7.38 ± 0.10) MeV. The simulation carried out in this study only uses one direction of irradiation. The use of gantries in practice allows irradiation to be carried out from various directions, so researchers want to see if irradiation from different directions can provide a better isodose rate.

2. Materials and Methods

Proton therapy modeling research uses computer hardware with the Windows operating system as the main component to run the MCNP6 software based on the Monte Carlo programming language FORTRAN. It is accompanied by other supporting software tools such as Visual Editor (Vised), Notepad++, Microsoft Excel, and Origin Pro 8.5. The simulation material used consists of a head and neck phantom (Fig. 1) referring to the ORNL-MIRD phantom, with the information for each part:

1. Head skull
2. Brain
3. Skeleton face
4. Spine
5. Soft tissue of head and neck
6. Scalp and neck skin
7. Environment outside the body

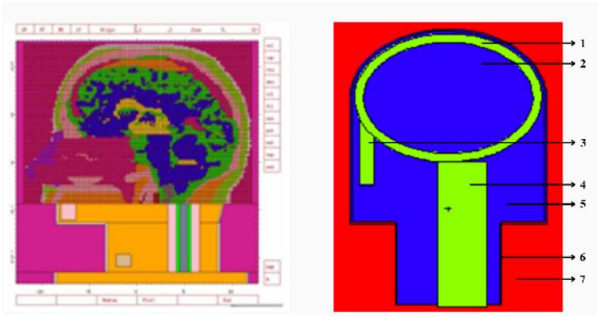

(a) (b)

Fig. 2: Head and neck phantom geometry in sagittal section (a) YZ [9] (Lazarine, 2006) and (b) simple geometry.

The initial stage of the simulation involves determining the optimal repetition value, called history cutoff (NPS), to obtain calculation results with a relatively constant relative error and a reasonable simulation time. The tumor or target cells are modeled in the form of a cube (Fig. 2(a)) with dimensions of 1.2×1.2×1.2 cm^3, located at a depth of 8 cm from the left, 9 cm from the right and 10.1 cm from the top of each surface of the head phantom geometry.

The target model is divided into 27 cubic partitions to achieve isodose distribution (Fig. 2(b)). As the irradiation area, the target cells are simulated as cubes to map the dose distribution received in each part of the target cells. The radiation source used in this simulation is a cylindrical proton particle, with the energy set in the range of 101 to 136 MeV according to the direction of the radiation source to obtain results close to the isodose.

The radiation source is positioned 20 cm away from the body surface. Irradiation is carried out using a pencil beam collimator with a diameter of 0.4 cm. Dose calculations with three directions of radiation source are performed step by step through one direction (right, left, and above), two directions (right-above, left-above, and right-left), and three directions of radiation (right-left-above) to obtain appropriate energy variations for each source direction. Irradiation is conducted at intervals of 0.1 cm for each to achieve uniform dose distribution and determine the optimal dose that can be obtained when irradiation is performed from various directions.

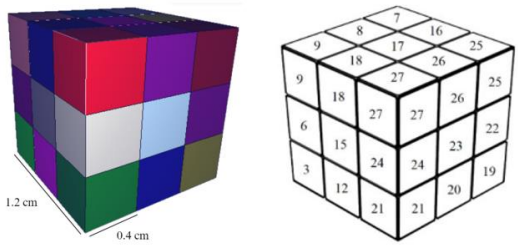

(a) (b)

Fig. 3: Visualization of (a) 3D and (b) cubic cell mapping geometric area of tumor cell irradiation.

The output results in the MCNP6 software are in units of MeV/gram. This differs from the International System of Units (SI) used in radiation dose calculations, which is gray (Gy) or joule per kilogram for absorbed dose and sievert (Sv) for effective and equivalent dose. Therefore, conversion is necessary to determine the actual dose magnitude using the following equation:

$$1\,\frac{\text{MeV}}{\text{gram}} = \frac{(1\times10^{6})\times(1.6\times10^{-19})\ Joule}{1\times10^{-3}\ kg} \qquad (1)$$

3. Result and Discussion

3.1. Dose Distribution with a Single Direction Source

Irradiation with a single source from the right of the irradiation area is carried out with energy variations of 109.2 MeV, 113 MeV, 114.7 MeV, and 115 MeV. The radiation source is perpendicular to the center of the irradiation area, located at a depth of 8 cm from the surface of the phantom's geometry. As seen in the graph (Fig. 4), there are still fluctuations with a relative error of (2.39 ± 0.17) MeV/gram per proton, and the expected isodose value is indicated by the horizontal red line on the graph. Irradiation with a source from the right of the irradiation area shows an isodose level percentage of 83.47%. The highest dose is located in cube cell 5, with a dose of 3.21 MeV/gram per proton, and the lowest in cube cell 19, with a dose of 1.48 MeV/gram per proton. Table 1 shows the average pixel and netOD values for the variation of TPS dose values for red, green, and blue channels. While Figure 4 displays the relationship curve of pixel value and netOD as a function of TPS dose value. Irradiation with a single source from the left of the irradiation area is carried out with energy variations of 101 MeV, 107.4 MeV, 107.8 MeV, and 108.2 MeV.

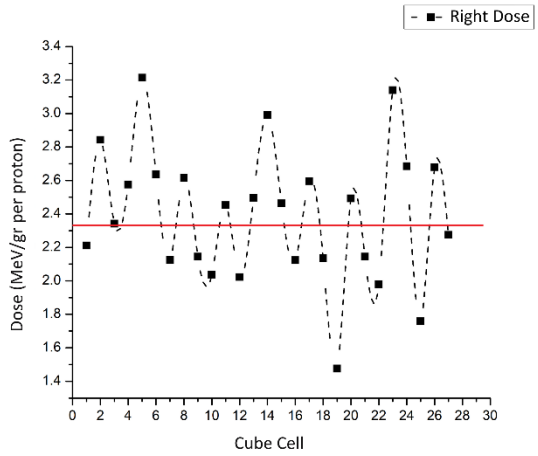

Fig. 4: Graph of proton dose distribution with irradiation from the right direction source.

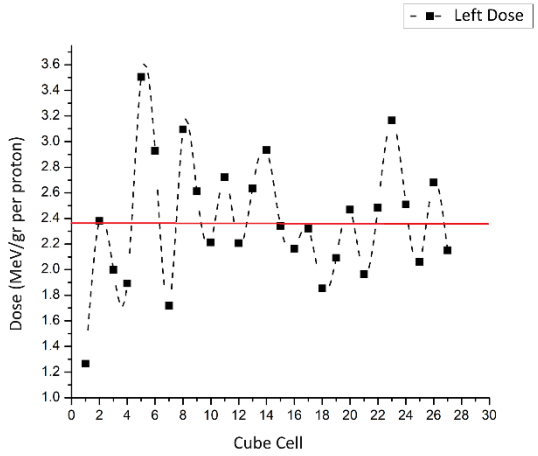

Fig. 5: Graph of proton dose distribution with irradiation from the left direction source.

The radiation source is perpendicular to the center of the irradiation area, located at a depth of 9.2 cm from the surface of the head phantom geometry. As seen in the graph (Fig. 5), there are still fluctuations with a relative error of (2.38 ± 0.34) MeV/gram per proton, and the expected isodose value is indicated by the horizontal red line on the graph. Irradiation with a source from the left of the irradiation area shows an isodose level percentage of 79.87%. The highest dose is located in cube cell 1, with a dose of 1.27 MeV/gram per proton, and the lowest in cube cell 5, with a dose of 3.50 MeV/gram per proton.

Irradiation with a single source from above the irradiation area is performed with energy variations of 134 MeV, 135.2 MeV, 135.4 MeV, and 135.7 MeV. When viewed from above, the irradiation area is located at a depth of 10.1 cm from the surface of the phantom's geometry. In the graph (Fig. 6), it is evident that there are still fluctuations with a relative error of (2.40 ± 0.01) MeV/gram per proton, as indicated by the horizontal red line, with an isodose level percentage of 47.53%. The highest dose is located in cube cell 20, with a dose of 4.98 MeV/gram per proton, and the lowest in cube cell 3, with a dose of 0.67 MeV/gram per proton.

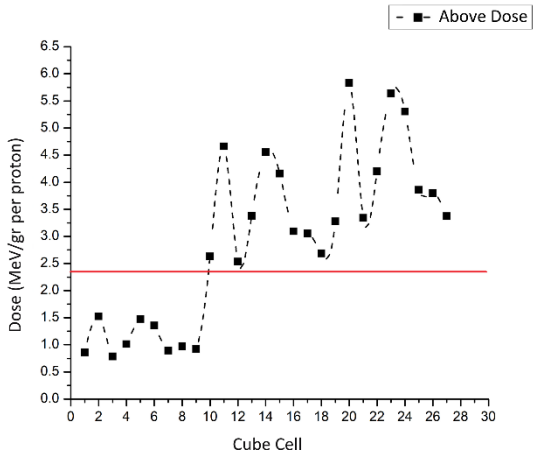

Fig. 6: Graph of proton dose distribution with irradiation from the above direction source.

3.2. Dose Distribution Two-Direction Source

Irradiation with a two-directional source from the right and above the irradiation area results in uneven energy distribution. The dose distribution graph (Fig. 7) shows fluctuations with a relative error of (4.79 ± 0.17) MeV/gram per proton, with an isodose level percentage of 71.95%. The highest dose is in cube cell 20, with a dose of 7.67 MeV/gram, and the lowest in cube cell 7, with a dose of 2.84 MeV/gram.

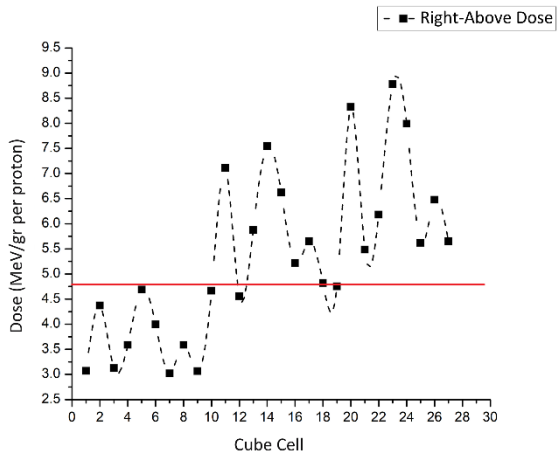

Fig. 7: Graph of proton dose distribution with two-direction radiation source from two-directional sources (right and above).

Irradiation with two sources from the left and above the irradiation area also results in uneven energy distribution. The dose distribution with a two-direction radiation source can be seen in the graph (Fig. 8). There are still fluctuations with a relative error of (4.78 ± 0.34) MeV/gram per proton with an isodose level of 69.60%. The highest dose is in cube cell 23, with a dose of 7.69 MeV/gram, and the lowest in cube cell 1, with a dose of 2.04 MeV/gram.

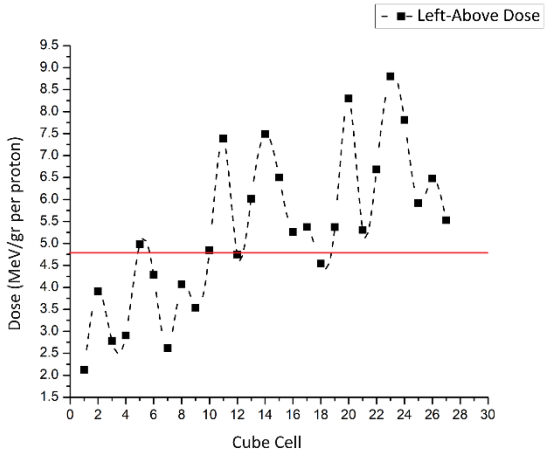

Fig. 8: Graph of proton dose distribution with two-direction radiation source from two-directional sources (left and above).

Irradiation from the left and above the irradiation area also results in uneven energy distribution (Fig. 9). As seen in Figure 4.28, there are still fluctuations with a relative error of (4.78 ± 0.50) MeV/gram per proton, with an isodose level percentage of 83.25%. The highest dose is in cube cell 5, with a dose of 6.72 MeV/gram, and the lowest in cube cell 1, with a dose of 3.48 MeV/gram.

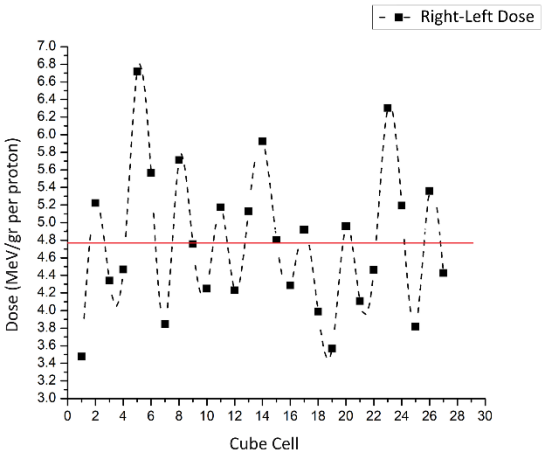

Fig. 9: Graph of proton dose distribution with two-direction radiation source from two-directional sources (right and left).

3.3. Dose Distribution Three-Direction Source

Irradiation with three sources from the right, left, and above the irradiation area (C) also results in uneven energy distribution. The dose distribution graph (Fig. 10) shows there are still fluctuations with a relative error of (7.18 ± 0.50) MeV/gram per proton, with an isodose level percentage of 77.57%. The highest dose is in cube cell 23, with a dose of 10.83 MeV/gram, and the lowest in cube cell 1, with a dose of 4.25 MeV/gram.

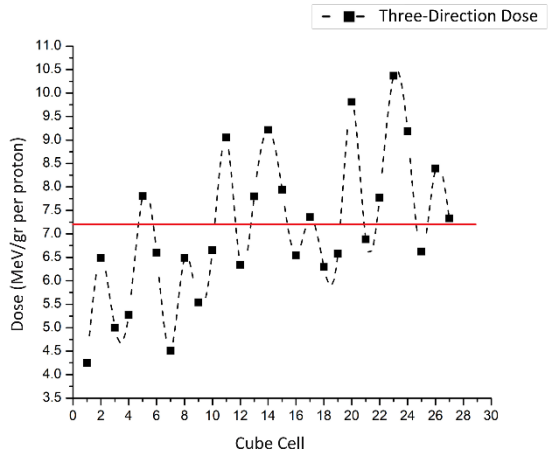

Fig. 10: Graph of proton dose distribution with three-direction radiation source from three-directional sources (right, left, and above).

Based on the results of dose distribution plotted on graphs with different radiation source directions, it is found that radiation dose distribution with a single source provides a relatively even dose distribution. Still, the magnitude of the dose received in each layer of the irradiation area varies significantly from the average dose or ideal dose for each cubic cell when viewed in terms of the x, y, and z axes. Dose distribution with two-direction radiation sources results in a reasonably uniform dose distribution, especially when irradiated from the right and left directions of the irradiation area. The dose magnitude received in each layer of the irradiation area approaches the average dose for each cubic cell.

The results of dose distribution with different radiation source directions yield different outcomes. Irradiation with a single-source direction from the right or left of the irradiation area provides a higher isodose level, as the radiation angles from both directions are relatively more parallel than the radiation angle when irradiation is performed from above the irradiation area. When the source position is perpendicular to the target, the received dose is large and gradually decreases as the distance from the target increases. The particle trajectories are parallel when the radiation source is perpendicular to the target, resulting in a higher dose. However, when the radiation direction is not parallel to the target, a limiting angle increases the radiation distance, and the dose decreases [10]. Theory regarding the relationship between energy and the track diameter or particle distance for non-normal incidence protons indicates that the track diameter decreases with increasing radiation angle [11]. This results in the highest dose being received in the central part of the irradiation area.

The tally results obtained using MCNP are in MeV/gram units, so a conversion factor is required to get the unit of absorbed dose. Absorbed dose in SI units is defined in gray (Gy), where 1 Gy is equivalent to 1 joule per kilogram, so the tally results in MeV/gram units can be converted to gray (Equation 1).

Table 1: Proton doses received by tumor cells

Source Direction	*Tally* F6 (MeV/gram per proton)	Absorbed Dose (nGy/s)
A1	2.39 ± 0.17	23.95 ± 0.03
A2	2.38 ± 0.34	23.83 ± 0.06
A3	2.40 ± 0.11	24.00 ± 0.02
B1	4.79 ± 0.17	47.94 ± 0.03
B2	4.78 ± 0.34	47.83 ± 0.06
B3	4.77 ± 0.49	47.78 ± 0.08
C	7.18 ± 0.50	71.78 ± 0.08

The dose calculated by MCNP represents the dose per incoming proton, so in this study, the measured absorbed dose is in units of Gray per proton [12]. In addition to determining the conversion factor, a multiplication factor should be calculated to obtain the dose rate in Gy/s units [11].

3.4. Total Dose to The Tumor Cells

In addition to examining the proton dose distribution, this study was also conducted to investigate the distribution of secondary doses, such as photons, neutrons, and electrons. The secondary doses in this experiment have minimal values on the order of 10-5. The magnitude of the dose received by the tumor cells can be seen in Table 2. Based on the calculations, it is known that the highest dose is obtained when irradiation is performed from three radiation source directions and the lowest dose is obtained when irradiation is done from a single radiation source direction from the left.

Table 3: Total dose received by healthy cells relative to the dose of tumor cells.

Healthy Organ	Source Direction	Dose (MeV/gram per proton)
Brain	A1	0.30 ± 0.00
	A2	0.24 ± 0.00
	A3	0.80 ± 0.00
	B1	1.10 ± 0.00
	B2	1.04 ± 0.00
	B3	0.54 ± 0.00
	C	1.34 ± 0.00
Skull	A1	0.01 ± 0.00
	A2	0.10 ± 0.00
	A3	0.06 ± 0.00
	B1	0.16 ± 0.00
	B2	0.17 ± 0.00
	B3	0.20 ± 0.00
	C	0.26 ± 0.00
Skeleton Face	A1	0.02 ± 0.00
	A2	0.02 ± 0.00
	A3	0.00 ± 0.10
	B1	0.02 ± 0.10
	B2	0.02 ± 0.10
	B3	0.05 ± 0.01
	C	0.05 ± 0.10
Spine	A1	0.00 ± 0.03
	A2	0.00 ± 0.04
	A3	0.00 ± 0.11
	B1	0.00 ± 0.12
	B2	0.00 ± 0.12
	B3	0.00 ± 0.05
	C	0.00 ± 0.12
Soft tissue	A1	0.01 ± 0.00
	A2	0.02 ± 0.00
	A3	0.00 ± 0.00
	B1	0.02 ± 0.00
	B2	0.02 ± 0.00
	B3	0.03 ± 0.00
	C	0.03 ± 0.00
Skin	A1	0.02 ± 0.00
	A2	0.02 ± 0.00
	A3	0.02 ± 0.00
	B1	0.04 ± 0.00
	B2	0.04 ± 0.00
	B3	0.03 ± 0.00
	C	0.05 ± 0.00

Table 2: The total dose received by tumor cells.

Source Direction	Dose (MeV/gram per proton)				
		(10^{-5})			Total
	p	γ	*n*	*e*	
A1	2.39 ± 0.17	4.13 ± 0.12	1.25 ± 1.21	2.00 ± 0.74	2.39 ± 0.17
A2	2.38 ± 0.34	3.86 ± 0.13	1.64 ± 1.41	1.94 ± 0.80	2.38 ± 0.34
A3	2.40 ± 0.11	3.71 ± 0.12	1.49 ± 1.38	2.11 ± 0.74	2.40 ± 0.11
B1	4.79 ± 0.17	7.83 ± 0.17	2.74 ± 1.85	4.11 ± 1.01	4.79 ± 0.17
B2	4.78 ± 0.34	7.57 ± 0.18	3.12 ± 1.99	4.05 ± 0.17	4.78 ± 0.34
B3	4.77 ± 0.49	7.99 ± 0.18	2.89 ± 1.87	3.94 ± 1.10	4.77 ± 0.49
C	7.18 ± 0.50	11.70 ± 0.22	4.38 ± 2.34	6.05 ± 1.33	7.18 ± 0.50

3.5. Total Dose to Healthy Organs

The doses of healthy organs in the simulation are compared to the Organ At Risk (OAR) tolerance values to determine whether the radiation doses are within safe limits. The allowable dose limits in therapy simulations and references vary for each treatment planning. Determining the allowable OAR dose limit is 1% of the dose used in the therapy process [13].

The magnitude of the dose received by healthy organs in this simulation is relatively small compared to that of tumor cells. Based on the data obtained (Table 3), it can be concluded that most of the doses received by healthy organs have met the OAR dose limits.

4. Conclusions

The proton dose distribution in proton therapy for Kraniofaringioma tumor with a single radiation source direction results in isodose levels of 83.47% from the right, 79.87% from the left, and 47.53% from above. Two-direction radiation sources yield isodose levels of 71.95% from right-above, 69.60% from left-above, and 83.25% from right-left. Subsequently, radiation from the right-left-above sources results in an isodose level of 77.57% for the three-direction radiation source.

The total absorbed dose received by the tumor cells for a single radiation source direction from the right is (2.4 ± 0.2) MeV/gram per proton, from the left is (2.4 ± 0.3) MeV/gram per proton, and from above is (2.4 ± 0.1) MeV/gram per proton. With two-direction radiation sources from right-above, it provides a total absorbed dose of (4.8 ± 0.2) MeV/gram per proton, from left-above is (4.8 ± 0.3) MeV/gram per proton, and from right-left irradiation area is (4.8 ± 0.5) MeV/gram per proton. Three-direction radiation sources from the right-left-above irradiation area provide a dose of (7.2 ± 0.5) MeV/gram per proton. The magnitude of the total absorbed dose received by healthy organs ranges from 0% to 1.23% relative to the total dose received by the tumor cells.

Acknowledgments

Acknowledgments are expressed to the members of the Theory and Computation Research Group, Department of Physics, Sebelas Maret University and Mr. Fajar Arianto and Mr. Azizul Khakim for providing the MCNP6's license, and people who cannot be fully mentioned in this paper.

References

[1] H. L. Muller, "The Diagnosis and Treatment of Craniopharyngioma" Neuroendocrinology, 110, 753–766, (2020).

[2] R. Prieto, M. Rosdolsky, V. Hofecker, L. Barrios, & J. M. Pascual, "Craniopharyngioma treatment: An updated summary of important Clinicopathological concepts" Expert Review of Endocrinology and Metabolism, 15(4), 261–282, (2020).

[3] P. Li, J. Wang, A. Axier, K. Zhou, J. Yun, H. Wang, T. Zhang, & S. Li, "Proton therapy for craniopharyngioma in adults: A protocol for systematic review and meta-analysis" BMJ Open, 11, 1–5, (2021).

[4] R. H. Press, R. L. Bakst, S. Sharma, R. Kabarriti, M. K. Garg, B. Yeh, D. Y. Gelbum, & N. Y. Lee, "Clinical review of proton therapy in the treatment of unilateral head and neck cancers" International Journal of Particle Therapy, 8, 248–260, (2021).

[5] S. S. James, C. Grasberger, & H. M. Lu, "Consideration when Treating Lung Cancer with Passive Scatter or Active Scanning Proton Therapy" Translational Lung Cancer Research, 7, 210-215, (2018).

[6] R. Mutamimah, Susilo, & Y. Sardjono, "Aplikasi Program PHITS Versi 3.21 untuk Analisis Dosis Radiasi pada Terapi Otak dengan Metode Proton Therapy" UPEJ, 11, 26-35, (2022).

[7] Z. Y. Yang, P. H. Tsai, S. C. Lee, C. C. Chen, T. Sato, & R. J. Sheu, "Inter-comparison of Dose Distribution Calculated by FLUKA, GEANT4, MCNP, and PHITS for Proton Therapy" EPJ Web of Conference, 153.04011, (2017).

[8] K. N. Widyanti, Chonsin, Widodo, & Bunawas, "Studi Distribusi Fluks Neutron Termal dan Energi yang Dihasilkan Linac menggunakan Detektor CR-39 pada Medium Air" NATURAL, 4, 145-152, (2018).

[9] A. W. Putri, "Penentuan Energi Proton Paling Optimal untuk Terapi Proton dengan Model Kolimator Penci Beam pada Tumor Kraniofaringima menggunakan Perangkat Lunak MCNP6" Skripsi, Surakarta, Universitas Sebelas Maret, (2022).

[10] R. M. Przybocki, Gatu Johnson, G. D. Sutcliffe, B. Lahmann, F. H. Seguin, J. A. Frenje, P. Adrian, T. M. Johnson, J. N. Pearcy, Kabadi, A. Birkel, & R. D. Petrasso, "Response of CR-39 Nuclear Track Detectors to Protons with Non-normal Incidence" Review of Scientific Instruments, 92, (2021).

[11] R. E. Susanto, E. Setiawati, F. Arianto, & P. Basuki, "Penentuan Faktor Koreksi Dosis Radiasi Sinar-X Linac 6 MV pada Ketidakhomogenan Jaringan Tubuh dengan MCNPX" Jurnal Ilmiah Aplikasi Isotop dan Radiasi, 18, 17-32, (2022).

[12] K. Kristiyanti, & E. Karyanta, "Analisis Dosis Radiasi pada Kolam Air Iradiator Gamma 2 MCi menggunakan MCNP" PRIMA, 11, 11-17, (2014).

[13] R. Poel, R. Rufenacht, E. Hermann, S. Scheib, P. Manser, D. M. Aebersold, & M. Reyes, "The Predictive Value of Segmentation Metrics on Dosimetry in Organ at Risk of the Brain" Medical Image Analysis, 73, 1-13, (2021).